CrossMark

Comparison of probabilistic and expert-based models in landslide susceptibility zonation mapping in part of Nilgiri District, Tamil Nadu, India

Balamurugan Guru[1] · Ramesh Veerappan[1] · Francis Sangma[1] · Somnath Bera[1]

Abstract In the present research work, the landslide susceptibility zonation (LSZ) mapping was carried out for the landslide prone area Nilgiri hills, Tamil Nadu, India. The LSZ mapping was carried out using ten landslide influencing factors along with extensive field investigation. The geospatial database was prepared through integrated remote sensing, geographical information systems, and GPS technologies. The methods adopted for the present study are frequency ratio (FR) which is probabilistic and analytical hierarchical process (AHP) which is subjective and objective based model. The FR values were evaluated through evaluating relationship between causative factors and past landslide (training) locations. The FR values were considered as the base for assigning the weights in AHP method along with the subjective knowledge. The final LSZ map were derived through the spatial integration of all causative factors and classified as different susceptibility classes viz. very low, low, moderate, high, and very high. The prediction accuracy of final LSZ map were validated using past landslide (validation) locations using area under curve (AUC) method. The FR model shown the highest prediction accuracy with AUC value of 0.6279, while the AHP model shown the AUC value of 0.5620.

✉ Balamurugan Guru
  gurubala.jtcdm@gmail.com

[1] Centre for Geoinformatics, Tata Institute of Social Sciences (TISS), Post Box No 8313, Deonar, Mumbai 400088, India

1 Introduction

Landslides cause serious threat to human life and damage to properties such as buildings, road network, etc. Landslides are commonly occurs in cut slopes of Ghat roads as well as natural slopes in the mountainous terrain. The natural hill slopes in the mountainous regions is highly altered by anthropogenic activities such as contruction of road network, urban growth, deforestation, and rapid land use modification, etc., may also influence the occurrence of landslides [1]. The mapping of landslide-prone zones in a region is essential for future planning and developmental activities. Landslide hazard/susceptibility and risk assessment has been getting comprehensive importance amongst the international scientific research community particularly in the field of geosciences [2]. Landslide susceptibility zonation (LSZ) mapping refers to the probability of future landslide occurrence in a region on the basis of correlation between causative factors with spatial distribution of past landslide locations. LHZ mapping differs from the susceptibility mapping in such a way, the temporal frequency (time recurrence) of a certain type and magnitude in a particular location within a set time is considered [3].

The landslide hazard or susceptibility assessment methods can be qualitative or quantitative [4]. The qualitative methods are subjective which describes the hazard zones in descriptive terms. The input data are generally derived either from field visits or by aerial photo interpretation. The qualitative methods can be divided into two

types viz. field geomorphological analysis and the integration of parameter maps. The field geomorphological analysis is made directly in the field based on the experience of the person who involved in the mapping [5]. The overlay analysis involves the identification and mapping of causative factors that influences the stability, assignment of weighted values to each class and each parameters based on the relative contribution to initiation of landslides, integration of parameter maps, and preparation of final landslide hazard or susceptibility map which shows varying hazard classes [6]. The quantitative methods include statistical analysis which can be bivariate [7] or multivariate [8] approaches, geotechnical engineering approaches [9], and artificial neural network analysis [10]. Probabilistic methods such as frequency ratio [11] and logistic regression [12] approaches were used in many research studies. Many studies were carried out using fuzzy logic [13, 14]. The analytical hierarchy process (AHP) method developed by [15] was applied widely to landslide studies [16].

In the present study, LSZ mapping was carried out in part of Nilgiris hills using frequency ratio (FR) which is complete statistical probabilistic method and analytical hierarchy process (AHP) which is subjective based multi-criteria method. The LSZ mapping of the study area were achieved with the help of remote sensing datasets, GIS tools and extensive field visit. The main objectives of the present study was to carry out LSZ mapping for the landslide prone area as well as to compare the resultant LSZ maps obtained by two different methods. Hence, the study reveals the impact of weightage deriving process in the final LSZ map. The LSZ map will be useful for administrators and planners for appropriate town planning in hilly terrain, to take necessary preventive and mitigation measures, and future developmental activities in this region.

2 Details of study area

The Nilgiri hill range is a part of Western Ghats situated in the North-Western part of State Tamil Nadu. The Nilgiri is one of the important tourist spots in the State. Ooty (is called "Queen of Hill Stations"), Coonoor, and Kotagiri are the three major hill stations located in this district. The district has an area of 2552 km^2, lying at an elevation of 1000–2633 m above mean sea level (amsl). The total population of this district as per the 2011 cencus was 0.735071 million. The present study covering the area of 672 km^2 and bounded by latitudes 11°15′–11°27′N and longitudes 76°37′–76°56′E (Fig. 1). The Nilgiri hill surrounded by the Coimbatore plains in the southeast, Bhavani plains in the northeast, Moyar valley in the north and Gudalur Plateau in the north-west. Moyar is an important river in the District and runs in an easterly direction, along

the northern boundary of the District. The drainage pattern is dendritic to radial and at places with outstanding rapids, cascades and waterfalls. The district usually receives rain both during south-west monsoon (Gudalur, Pandalur, Kundah and portion of Ooty Taluk) and north-east monsoon (Coonoor, Kotagiri, and Some portion of Ooty Taluks). The usual annual rainfall in this region varies from place to place and the range is somewhere between 1500 and 3000 mm.

In Nilgiri hills, the major landslide occurrences in the year 1978, 1993, 1995, 2002, 2007, and 2009, shows that the frequency of landslide occurrences increased in the study region [17]. The most devastation event that happened in the Nilgiris was in November 2009, when 45 people died [18]. The deforestation activity for growing vegetables and seasonal crops, tea and other plantation crops, which reduces the stability of the hill slope, leads to slope failures (Fig. 2). In Nilgiris, landslides are due to the effect of pore-pressure increase, particularly during the rainy seasons [19].

Geologically, the Charnockite Group, comprising of charnockite, two-pyroxene granulite, banded quartz-magnetite granulite/banded magnetite quartzite and thin pink quartzo-felspathic granulite are extensively developed in the north-eastern sector of the State and are well exposed in many prominent hill ranges such as Pallavaram–Chengleput, Javadi, Shevaroy, Chitteri, Kalrayan, Kollimalai, Pachchaimalai and Nilgiri [20]. The charnockite group of rocks with enclaves of Satyamangalam schist complex represented by charnockite and pyroxene granulite covers a major part of the district in the southern part, which is popularly known as ''Nilgiri Massif''. The Nilgiri Massif is capped by aluminous laterite at a number of places indicating the deep zone of weathering. Lenses and pockets of bauxite/bauxitic laterite, which are irregular in nature, occur in the high level laterite cappings over charnockite in the Nilgiri hills (1920–2530 m amsl), Nilgiri District. In the Nilgiri District bauxite occurrences can be grouped into three sectors, viz., Kotagiri, Ootacamund and Upper Bhavani.

3 Geospatial database of landslide influencing factors

In the present study various data sources such as the topographical map on 1:50,000 scale of the Survey of India (SOI), geological map published by the Geological Survey of India [21], Indian remote sensing (IRS) satellite ResourceSat2 LISS-IV satellite imagery with the spatial resolution of 5.8 m was procured from National Remote Sensing Centre (NRSC) and Advanced Spaceborne Thermal Emission and Reflection Radiometer (ASTER) digital
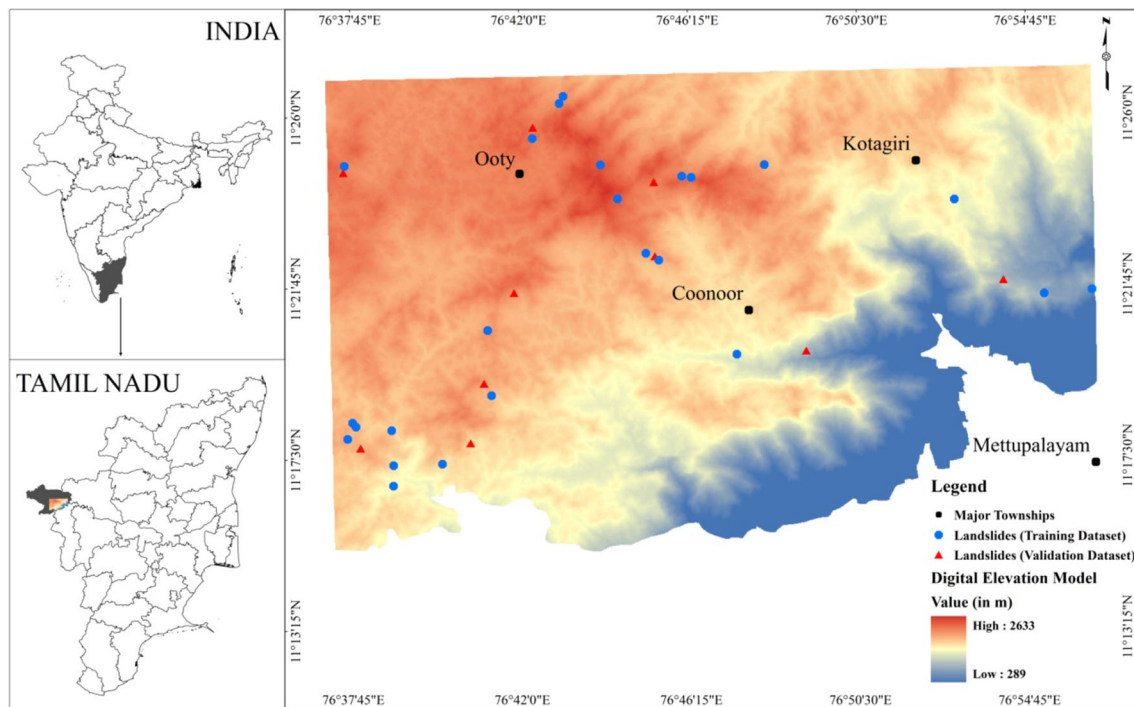
Fig. 1 Location map of the study area (part of Nilgiri hills)—Nilgiri District, Tamil Nadu, India

elevation model (DEM) data of 30 m resolution were used for the purpose of preparation of different thematic maps of diverse factors influences landslides. The ArcGIS 10.1 version software was used to prepare the thematic maps and its integration. There are no regulations available globally for selecting the landslide causative factors to prepare LSZ map [22]. The study on causative factors for LSZ mapping by [23] suggested that the parameters can be chosen on the basis of literature, data availability and experience, and technical reasons. In the present study, the different thematic layers of various causative factors considered for the study includes slope, slope aspect, slope curvature, elevation, lithology, land use and land cover, geomorphology, rainfall distribution, proximity to lineament, and proximity to drainage based on the knowledge about causes behind the past incidence of landslides in the study region as well as through review of literature on common landslide influencing factors. All the thematic maps were prepared in raster format with common pixel size of 10 m × 10 m.

3.1 Landslide inventory map

The landslide distribution map were prepared to evaluate the relationship between landslides and the causative factors, which will be helpful for the preparation of landslide susceptibility zonation (LSZ) maps and validation of the model [24]. The detailed landslide inventory or distribution

map of the study area was prepared by conducting field survey using handheld global positioning system (GPS) in the year 2015. The high resolution satellite imagery ResourceSat 2 was used to identify the landslide locations with the help of field GPS locations. There were 34 landslide locations identified in the study area and captured as point data layer (Fig. 1). The landslide inventory dataset was divided into training (24 landslide locations) and validation (10 landslide locations) dataset. The training landslide dataset was used to build the model, while the validation dataset was used to determine the prediction accuracy of the model adopted.

3.2 Topographical factors derived from DEM

The density and spatial extent of landslides is highly depends on the surface topography, which decides the flow sources and controls the direction of run-off [25]. ASTER DEM data was used to derive the topographical factors such as the slope, slope aspect, slope curvature and elevation. The factors were derived using the ArcGIS 10.1@ESRI spatial analyst tool.

3.2.1 Slope

The slope is one of the significant terrain factors which influences landslide in an area, because it controls the velocity of the surface and subsurface flows [26]. The slope

Fig. 2 Field photographs show
different land use practices
along hill slopes in the study
area: **a** builtup area and
agricultural land, **b** tea
plantation, **c** mixed-land use
practice
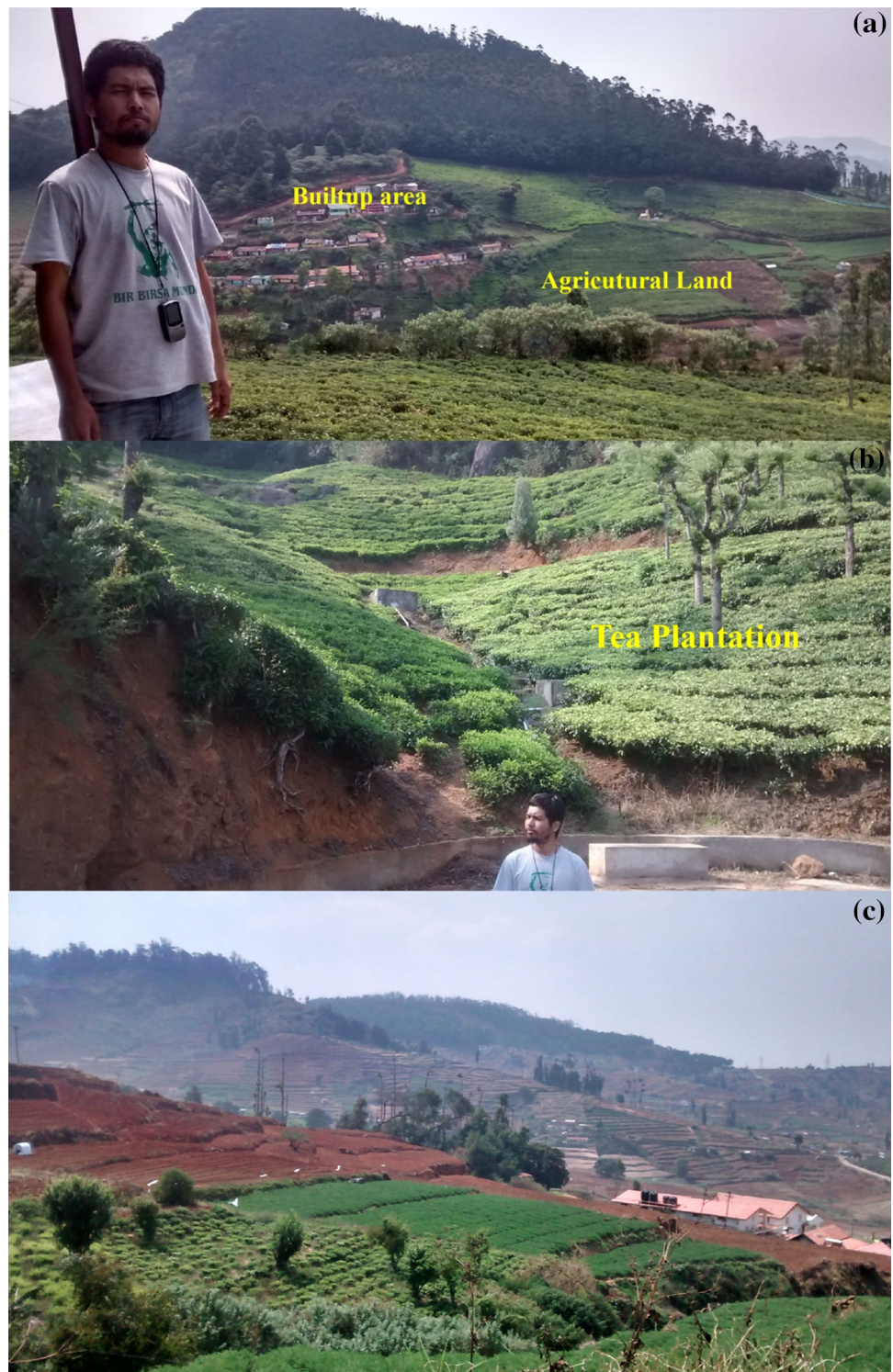
map (Fig. 3a) was derived from the DEM and reclassified
into five classes viz., < 10°, 10°–17°, 17°–25°, 25°–36°,
36°–74° respectively based on the Jenks natural breaks
classification [13, 24, 27].

3.2.2 Slope aspect

Slope aspect describes the direction of the slope face which
may get affected differently by sunlight, precipitation, and
wind. Hence, it indirectly affects the factors like soil moisture
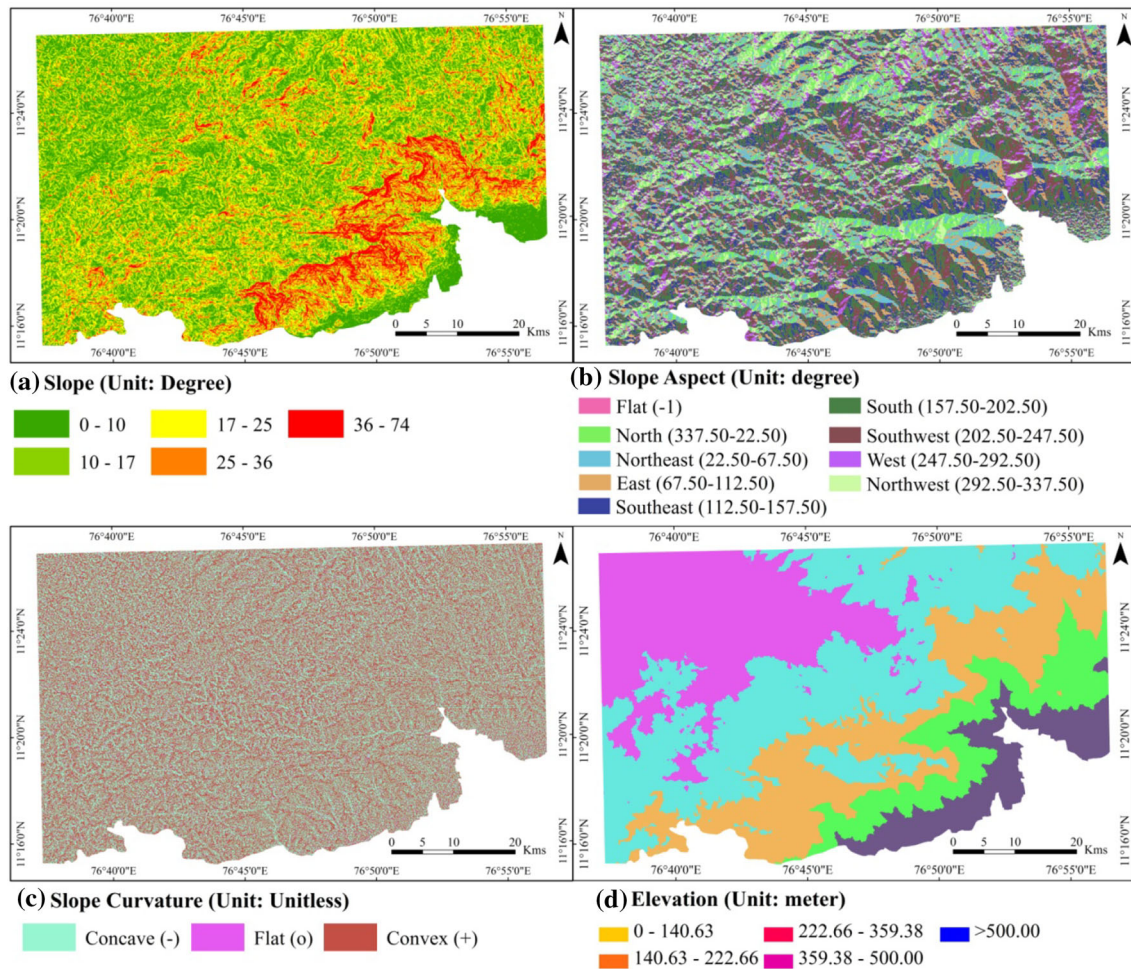and vegetation cover [28]. Aspect map was derived from

Fig. 3 Landslide causative factors: **a** slope, **b** slope aspect, **c** slope curvature, **d** elevation

DEM and reclassified into eight directional classes as North (337.5–22.5), Northeast (22.5–67.5), East (67.5–112.5), Southeast (112.5–157.5), South (157.5–202.5), Southwest (202.5–247.5), West (247.5–292.5), Northwest (292.5–337.5) respectively and one flat class with negative values (Fig. 3b).

3.2.3 Slope curvature

In the present study we considered combo curvature (combination of plane and profile), which helps us to study the morphology of the slope and flow of water across the surface [24]. The curvature map was derived from DEM and reclassified as concave (negative values), convex (positive values), and the zero values were classified as flat. The flat class in curvature indicates linear slope surface (Fig. 3c).

3.2.4 Elevation

The natural condition of the terrain gets affected by varying climatic conditions at higher altitudes. The elevation gives us the overview of lowest and highest elevation [13]. The elevation range of the study area is 289–2633 m amsl. The whole range was reclassified into five classes based on natural breaks classification, i.e. 289–734, 734–1314, 1314–1764, 1764–2065, and 2065–2633 m (Fig. 3d).

3.3 Geological, environmental, and triggering factors

3.3.1 Lithology

The withholding capacity of rocks to the erosion and weathering activities is the important aspect in controlling the stability of the slope [29]. The lithology map of the study area was prepared from the geological map published by Geological Survey of India [21]. Charnockite,

garnetiferous quartzofeldspathic gneiss, fissile hornblende-biotite gneiss, and ultramaffic rocks are the major lithological units exist in the study area (Fig. 4a).

3.3.2 Land use and land cover

The land use modifications along hill slopes like deforestation, agricultural and constructional activities leads to landslides [30]. The land use and land cover map was interpreted and vectorized using high resolution ResourceSat2 satellite image and using topographic sheet as reference. The different land use and land cover features interpreted and digitized includes evergreen forest, deciduous forest, scrub forest, barren land, agriculture field-crop, agricultural field-tea plantation, builtup area, water body (Fig. 4b). The modification of natural slope conditions for the agricultural activities such as crop and tea plantation are influencing much for the landslides in the study area.

3.3.3 Geomorphology

Geomorphology describes the terrain condition, which helps us to gain knowledge behind the development of landslide occurrence in an area [11, 31]. The

geomorphological features were visually interpreted with the aid of satellite image includes denudational hill, highly dissected structural hill, intermontane valley, and piedmont zone (Fig. 4c).

3.3.4 Rainfall distribution

The rainfall was considered as a triggering factor for landslide initiation. The annual average rainfall was calculated from the $0.5° \times 0.5°$ rainfall grid data. The rainfall distribution map was prepared by inverse distance weighted (IDW) spatial interpolation method and reclassified into five classes based on Jenks natural breaks classification viz. 1233–1430, 1430–1558, 1558–1695, 1695–1830, 1830–2028 mm (Fig. 4d).

3.3.5 Proximity to drainage

The distance from drainage to the source location of the landslides has varying influence on the initiation of landslides i.e. closer the distance higher the possibility of occurrences. The major streams and drainages were digitized from the SOI topographic sheet. Further, the proximity to drainage was calculated using Euclidean distance
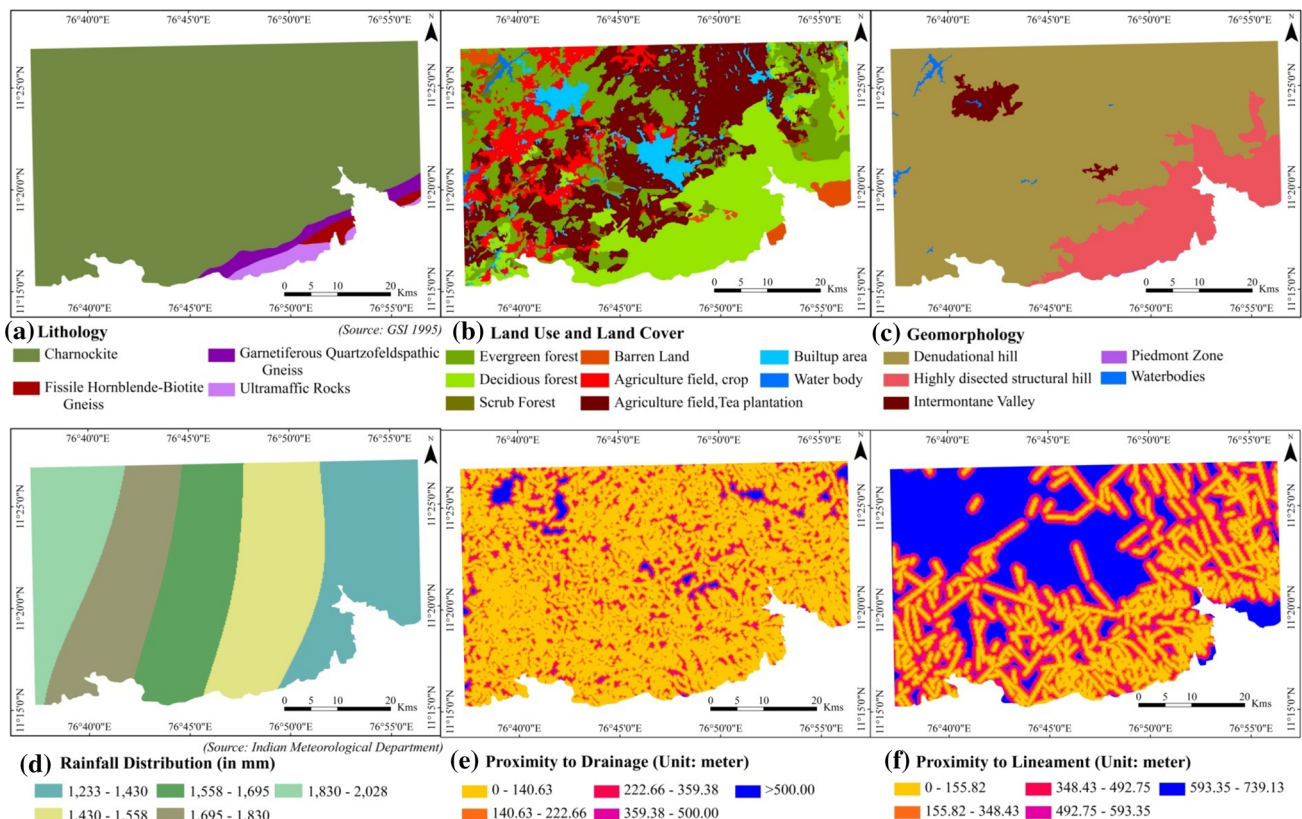

Fig. 4 Landslide causative factors: **a** lithology, **b** land use and land cover, **c** geomorphology, **d** rainfall distribution, **e** proximity to drainages, **f** proximity to lineaments

method in ArcGIS 10.1@ESRI and reclassified into five natural break classes viz. 0–140.625, 140.626–222.656, 222.657–359.375, 359.376–500.000, > 500 m (Fig. 4e).

3.3.6 Proximity to lineaments

The lineaments were visually interpreted from high-resolution satellite imagery, as the possible occurrences of landslides are likely to be high in regions that fall close [13]. The distance from lineament was calculated using Euclidean distance method in ArcGIS 10.1@ESRI. The proximity to lineament was reclassified into five natural break classes viz., 0–155.822, 155.823–348.428, 348.429–492.752, 492.753–593.352, 593.353–739.128 m (Fig. 4f).

4 LSZ mapping methods

4.1 Frequency ratio (FR) method

In the present study, the influence values of each class in the individual causative factors were obtained through frequency ratio (FR) method [32]. The relationship of past landslides to each influencing factor can be calculated using FR method. The FR value greater than 1 means higher correlation which indicates higher the possibility of landslide occurrence. The FR value of each class in individual causative factor was calculated using the Eq. 1. Further, the FR values of each causative factor were summed up to get the final landslide susceptibility index (LSI) value in each cell which indicates degree of landslide susceptibility, using the Eq. 2 [24].

$$\text{Frequency ratio} = \frac{\text{slide ratio}}{\text{class ratio}} \quad (1)$$

where slide ratio is the number of landslide pixels in a class to total number of landslide pixels; class ratio is the number of pixels in individual class to total number of pixels in a whole class

$$\text{LSI} = \Sigma\text{FR} \quad (2)$$

where LSI is landslide susceptibility index; FR is frequency ratios of each causative factor

4.2 Analytical hierarchy process (AHP) method

In the present study, analytical hierarchy process (AHP) which is a multi-criteria decision making (MCDM) approach developed by [15], was adopted to estimate the weights of the factors and ratings of the class in each landslide influencing factor through pair-wise comparison matrix on the basis of scale of preference given by [15].

The scale of preference (Table 1) ranges from 1 (equal preference) to 9 (extremely high preference) to the intersecting cell in the pair-wise comparison matrix of each influencing factor/classes under comparison against other factor/classes [33]. In the pair-wise comparison matrix, if the factor/class on the vertical axis has higher degree preference than the horizontal axis, at that time the scale given between 1 and 9. In opposition, if the factors/class on the horizontal axis of the matrix has having higher degree preference than the vertical axis, the scale considered in the reciprocals (1/2–1/9) [34]. In AHP method, the scale of preference can be decided based on the subjective, objective, and combination of both [35]. In the present study, the scale of preference was decided based on the subjective and objective method. The values assigned on the basis of presence of landslides in the classes of a parameter as well as subjective knowledge. The effect of subjectivity i.e. inconsistency can be estimated through the evaluation of consistency index (CI) using the Eq. 3 and consistency ratio (CR) using Eq. 4 [34].

$$CI = \frac{(\lambda_{max} - n)}{(n - 1)} \quad (3)$$

$$CR = \frac{CI}{RI} \quad (4)$$

where λ_{max} is the maximum eigen value; n is the number of causative factors present in the pair-wise comparison matrix.

CR can be calculated by ratio CI/RI, where RI stands for random index based on number of random samples [34] (Table 2). In the pair-wise comparison matrix, CR > 0.1 means there exists inconsistency and requires revision in the scale of preference [36]. The landslide susceptibility index (LSI) was calculated by adding all the scores obtained by multiplying weight of factor with rating of class as given in Eq. 5 [37].

Table 1 Scale of preference between two factors in AHP suggested by [15]

Numerical scales	Degree of preferences
1	Equal importance
3	Moderate dominance of one over another
5	Strong or essential dominance
7	Very strong or show dominance
9	Extremely high dominance
2, 4, 6, 8	Intermediate values
Reciprocals	For opposite comparison

Table 2 Random Index values for the pairwise comparisons in AHP analysis (after [34])

N	1	2	3	4	5	6	7	8	9	10
RI	0	0	0.58	0.90	1.12	1.24	1.32	1.41	1.45	1.49

$$LSI = \sum_{j=1}^{n}(W_j w_{ij}) \qquad (5)$$

where LSI is the landslide susceptibility index, W_j is the weight value of causative factor j, w_{ij} is the weight value of class i in causative factor j, and n is the number of causative factors.

5 Results and discussion

The FR values were evaluated based on the Eq. 1 and the results are presented as supplementary material Table S1. The results depicts that, the topographical factors like slope (17°–25° and 25°–36°), slope aspect classes (north, southeast, northwest, east), convex slope, elevation ranges (734–1314, 1764–2065, 2065–2633 m) possess greater than 1 FR values and indicating the higher correlation than the other classes present in topographical factors. Charnockite class in lithology; builtup area, agricultural field-crop and tea plantation in LULC, denudational class in geomorphology; 0–140.625 m distance from drainage and 0–155.822 m distance from lineaments are having higher correlation with past landslide locations. The hierarchically ordered causative factors and its pair-wise comparison to evaluate the normalized weights are given in

Table 3. Similarly, the pair-wise comparison of classes within the individual factors were evaluated and presented as supplementary material Table S2. The maximum eigen value, consistency index (CI), random index (RI), consistency ratio (CR) were also presented in the respective places in both the tables. The final score of the individual classes were calculated by multiplying the rating values of individual class with weight of individual factors.

## 5.1 Geospatial integration: LSZ mapping

In the present study, we have processed and converted all the vector based thematic layers into raster format to match the nominal spatial resolution 10 m pixel size of IRS-LISS-IV multispectral satellite imagery using the spatial analysis tool in ArcGIS 10.1 software. Geospatial database of all the considered landslide influencing factors were converted into raster format using the respective FR values and scores calculated using the AHP method. The spatial integration of all the raster layers was carried out through raster calculator tool in ArcGIS 10.1 software. The final landslide susceptibility index (LSI) values were evaluated using the Eqs. 2 and 5. The statistics of LSI values using the FR model results the minimum (3.28), maximum (17.11), mean (10.00), and standard deviation (1.83) values. The LSI output of AHP method depicts the minimum, maximum, mean, and standard deviation values 0.07, 0.43, 0.21, and 0.05, respectively. The integrated LSI values range were reclassified using natural breaks into five susceptibility classes qualitatively viz. very high, high, moderate, low and very low (Fig. 5a, b). The resultant landslide susceptibility classes indicate that each class having some importance in the future landslide occurrences. The past landslide locations were integrated with reclassified LSZ

Table 3 Pair-wise comparison matrix between the landslide influencing factors

| Conditioning factors	1	2	3	4	5	6	7	8	9	10	Normalized weights
Lithology (1)	1										0.02
Geomorphology (2)	2	1									0.02
Slope curvature (3)	3	2	1								0.03
Elevation (4)	4	3	2	1							0.04
Proximity to lineament (5)	5	4	3	2	1						0.06
Slope aspect (6)	6	5	4	3	2	1					0.08
Proximity to drainage (7)	7	6	5	4	3	2	1				0.11
Rainfall distribution (8)	8	7	6	5	4	3	2	1			0.15
Land use land cover (9)	9	8	7	6	5	4	3	2	1		0.21
Slope (9)	9	9	8	7	6	5	4	3	2	1	0.29

Maximum Eigen value: 10.85; consistency index (CI) = 0.09; random index (RI) = 1.49; consistency ratio (CR) = 0.06

Fig. 5 Landslide susceptibility maps: **a** frequency ratio, **b** analytical hierarchical process models
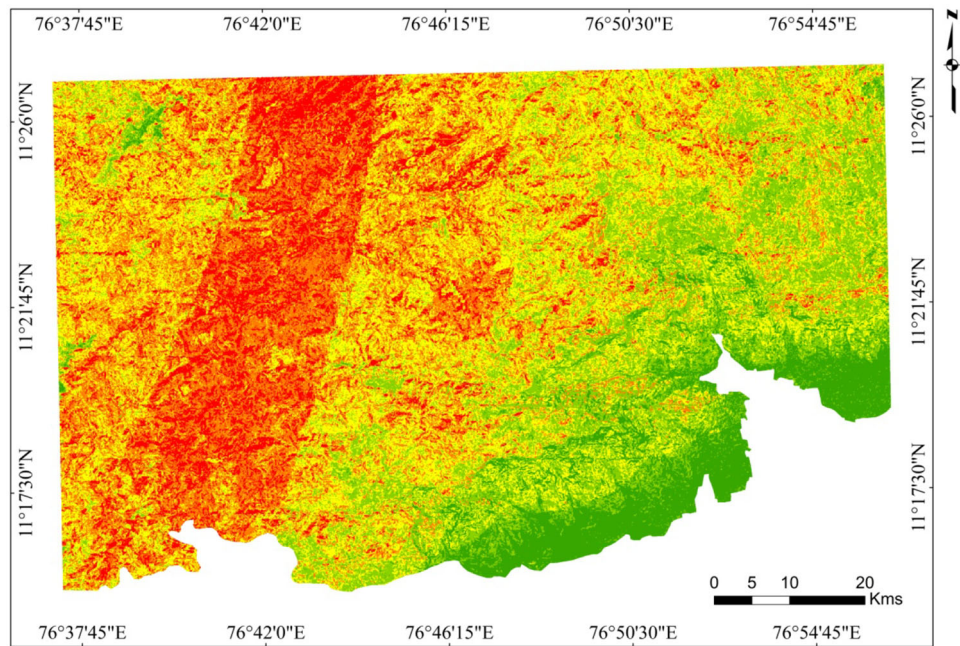
(a) Landslide Susceptibility Index (LSI) - FR Model

- Very Low (3.28 - 7.35)
- Low (7.35 - 9.15)
- Moderate (9.15 - 10.54)
- High (10.54 - 12.02)
- Very High (12.02 - 17.11)
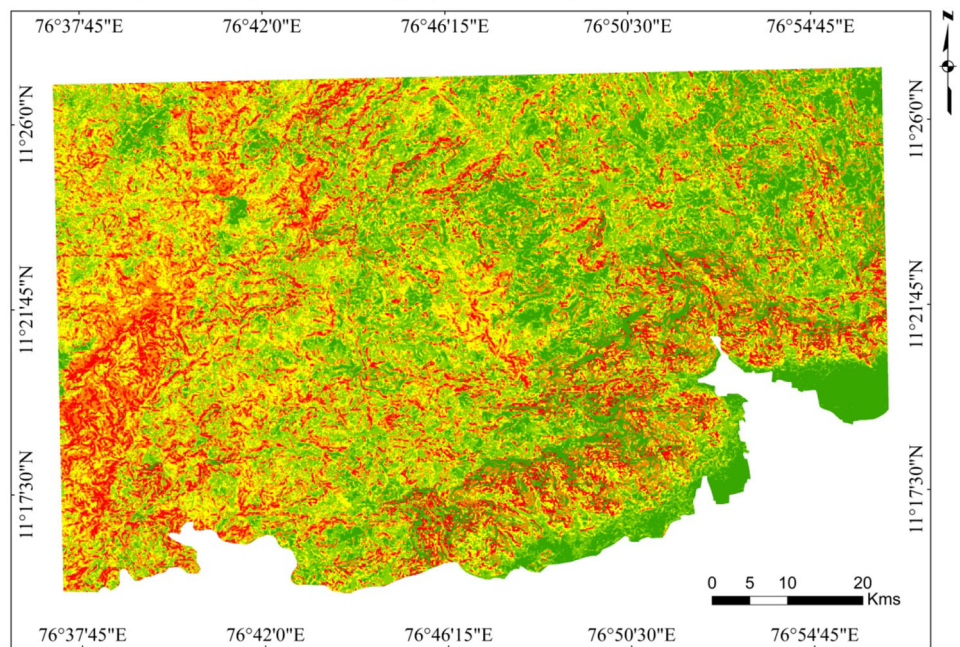
(b) Landslide Susceptibility Index (LSI) - AHP Model

- Very Low (0.071 - 0.16)
- Low (0.16 - 0.20)
- Moderate (0.20 - 0.24)
- High (0.24 - 0.28)
- Very High (0.28 - 0.43)

map prepared by FR and AHP methods, to determine the percentage of landslides within individual susceptibility classes. In the FR method, 62.50 and 20.83% of past landslide locations fall in very high and high susceptibility classes respectively, whereas in AHP method it was 37.50 and 29.17%, respectively as given in the Table 4.

Table 4 Percentage of past landslide (training) locations identified in the different landslide susceptibility classes of LSZ map prepared by the frequency ratio and analytical hierarchical process models

Landslide susceptibility class	No. of pixels in class	% of class pixels	No. of landslides in class	% of landslide pixels in class
Frequency ratio (FR) model				
Very high	810,072	12.05	15	62.50
High	1,858,428	27.64	5	20.83
Moderate	2,165,144	32.20	3	12.50
Low	1,296,668	19.28	1	4.17
Very low	594,176	8.84	0	0.00
Analytical hierarchical process (AHP) model				
Very high	796,296	11.84	9	37.50
High	1,115,917	16.59	7	29.17
Moderate	1,755,242	26.10	5	20.83
Low	1,862,989	27.70	3	12.50
Very low	1,194,044	17.76	0	0.00

Fig. 6 Graphical representation **a** success rate curves with AUC value derived using the landslide susceptibility index rank percentage and cumulative percentage of landslide (training) occurrence, **b** prediction rate curves with AUC value derived using the landslide susceptibility index rank percentage and cumulative percentage of landslide (validation) occurrence
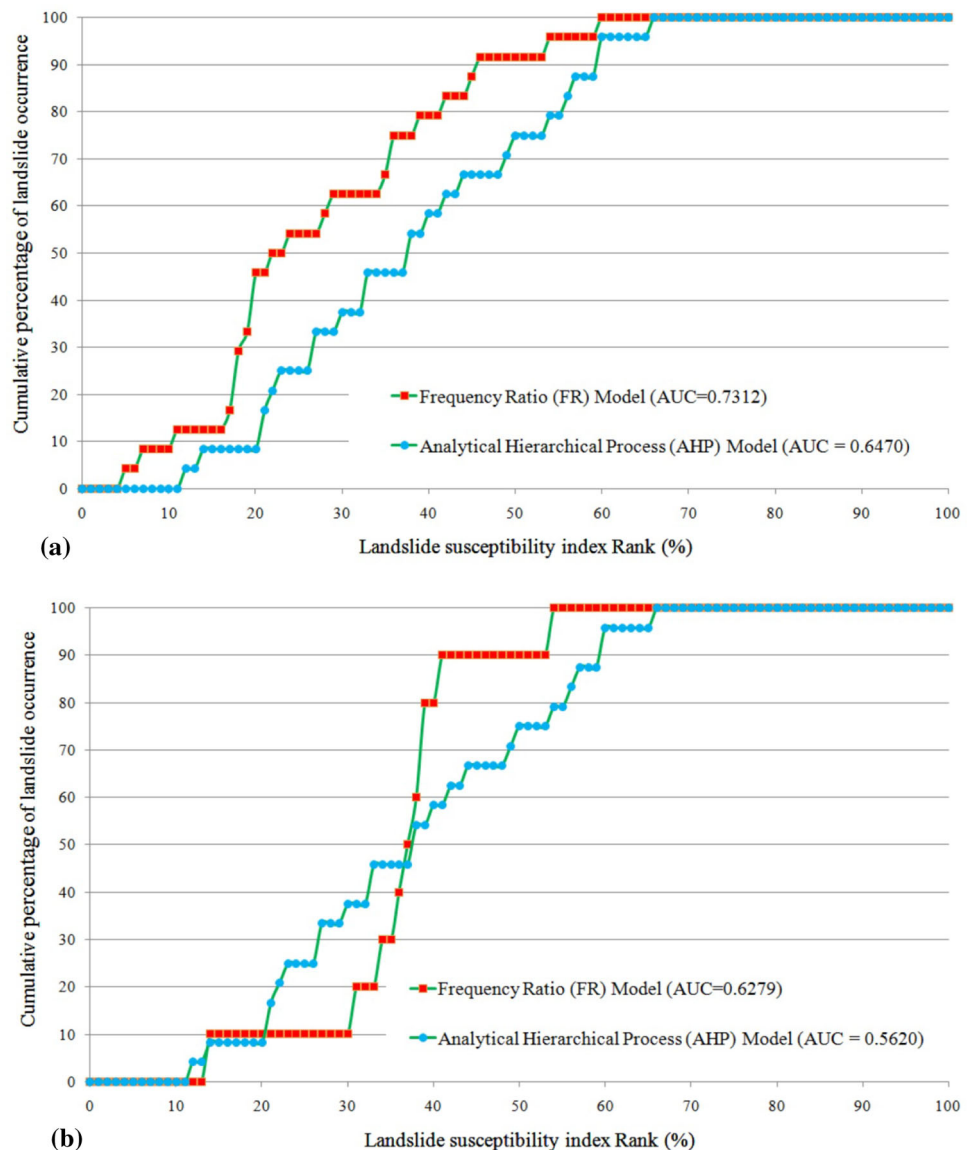
5.2 Comparison and validation

The LSZ map was prepared by FR and AHP methods were validated using the Area Under Curve (AUC) method, which determines the prediction capability of model adopted [38]. In the present study, the success rate and prediction rate curves were derived to validate the LSZ maps. To determine the success rate and prediction rate of the model adopted, AUC method has been globally used by many researchers [39]. The AUC value near to 1.0 indicates the higher accuracy of the model, while the value close to 0.5 reflects the inaccuracy of the model [40]. To draw the success and prediction rate curve and determine the AUC value, the LSI value of both the models were reclassified into 100 classes and ordered in the descending order. Then the percentage of the pixels covered in the each class was calculated. Further, training and validation landslide dataset were intersected with 100 classes to identify the percentage of landslide pixels fall in individual class. Finally, the cumulative percentage of training landslides (success rate) and validation landslides (prediction rate) occurrence in each class were evaluated. The AUC value of success rate curve (Fig. 6a) for the FR and AHP models were evaluated using training landslide dataset as 0.7312 and 0.6470, respectively. The AUC value of prediction rate curve (Fig. 6b) for the FR and AHP models were evaluated using validation landslide dataset as 0.6279 and 0.5620, respectively, reveals that the FR model shows the higher prediction accuracy than the AHP model for the chosen study area. The higher prediction accuracy of FR method is due to weight deriving process in which the influence of each class was derived based on the relationship with past landslide occurrences. However, AHP method results less prediction accuracy due to the fact that the weight deriving process involved more subjectivity.

6 Conclusions

The present research work was carried out with the aim of performing LSZ mapping and to prove the application of probabilistic and subjective based method in LSZ mapping. The remote sensing, GIS, and GPS techniques were helpful in preparing the geospatial database of landslide influencing factors considered for the present study. In terms prediction accuracy, the AUC value of Frequency Ratio (FR) model was 0.6279, while the Analytical Hierarchical Process (AHP) model given the AUC value of 0.5620. The study depicts that the FR method has the higher prediction accuracy than the AUC model in the present study.

Compliance with ethical standards

Conflict of interest On behalf of all authors, the corresponding author states that there is no conflict of interest.

References

1. Das, I., Stein, A., Kerle, N., & Dadhwal, V. K. (2011). Probabilistic landslide hazard assessment using homogeneous susceptible units (HSU) along a national highway corridor in the northern Himalayas, India. *Landslides, 8,* 293–308.
2. Van Westen, C. J., van Asch, T. W. J., & Soeters, R. (2006). Landslide hazard and risk zonation—Why is it still so difficult? *Bulletin of Engineering Geology and the Environment, 65*(2), 167–184.
3. Varnes, D. J. (1984). *Landslide hazard zonation: A review of principles and practice* (pp. 1–63). International Association of Engineering Geology, UNESCO, Paris.
4. Guzzetti, F., Carrara, A., Cardinalli, M., & Reichenbach, P. (1999). Landslide hazard evaluation: a review of current techniques and their application in a multi-case study, central Italy. *Geomorphology, 31,* 181–216.
5. Rupke, J., Cammeraat, E., Seijmonsbergen, A. C., & van Westen, C. J. (1988). Engineering geomorphology of Widentobel Catchment, Appenzell and Sankt Gallen, Switzerland: a geomorphological inventory system applied to geotechnical appraisal of slope stability. *Engineering Geology, 26,* 33–68.
6. Stevenson, P. C. (1977). An empirical method for the evaluation of relative landslide risk. *Bulletin of International Association of Engineering Geology and the Environment, 16,* 69–72.
7. Pradhan, B., & Lee, S. (2010). Landslide susceptibility assessment and factor effect analysis: backpropagation artificial neural networks and their comparison with frequency ratio and bivariate logistic regression modeling. *Environmental Modeling & Software, 25*(6), 747–759.
8. Shahabi, H., Ahmad, B., & Khezri, S. (2012). Evaluation and comparison of bivariate and multivariate statistical methods for landslide susceptibility mapping (case study: Zab basin). *Arabian Journal of Geosciences, 6*(10), 3885–3907.
9. Singh, R., Umrao, R. K., & Singh, T. N. (2014). Stability evaluation of road-cut slopes in the Lesser Himalaya of Uttarakhand, India: conventional and numerical approaches. *Bulletin of Engineering Geology and the Environment, 73*(3), 845–857.
10. Choi, J., Oh, H. J., Lee, H. J., Lee, C., & Lee, S. (2012). Combining landslide susceptibility maps obtained from frequency ratio, logistic regression, and artificial neural network models using ASTER images and GIS. *Engineering Geology, 124,* 12–23.
11. Kannan, M., Saranathan, E., & Anbalagan, R. (2013). Landslide vulnerability mapping using frequency ratio model: A geospatial approach in Bodi-Bodimettu Ghat section, Theni district, Tamil Nadu, India. *Arabian Journal of Geosciences, 6*(8), 2901–2913.
12. Akbari, A., Yahaya, F. B. M., Azamirad, M., & Fanodi, M. (2014). Landslide susceptibility mapping using logistic regression analysis and GIS tools. *Electronic Journal of Geotechnical Engineering, 19,* 1687–1696.
13. Balamurugan, G., Ramesh, V., & Touthang, M. (2016). Landslide susceptibility zonation mapping using frequency ratio and fuzzy

gamma operator models in part of NH-39, Manipur, India. *Natural Hazards, 84*(1), 465–488.

14. Hinotoli, V. Sema, Guru, Balamurugan, & Veerappan, Ramesh. (2017). Fuzzy gamma operator model for preparing landslide susceptibility zonation mapping in parts of Kohima town, Nagaland, India. *Modelling Earth Systems and Environment, 3*(2), 499–514.

15. Saaty, T. L. (1977). A scaling method for priorities in hierarchical structures. *Journal of Mathematical Psychology, 15*(3), 234–281.

16. Ramesh, V., Ankur, N., & Anbazhagan, S. (2017). Landslide susceptibility mapping and comparison using frequency ratio and analytical hierarchy process in part of NH-58, Uttarakhand, India. In M. Mikos, B. Tiwari, Y. Yin & K. Sassa (Eds.), *Advancing culture of living with landslides—Volume 2 advances in landslide science* (pp. 1081–1091).

17. Vasantha Kumar, S., & Bhagavanulu, D. V. S. (2008). Effect of deforestation on landslides in Nilgiris District—A case study. *Journal Indian Society of Remote Sensing, 36,* 105–108.

18. Dominique, B. (2014, July 23). Nilgiris most landslide-prone in south: Expert. *The Times of India City.* Retrieved from http://timesofindia.indiatimes.com/city/chennai/Nilgiris-most-landslide-prone-in-south-Expert/articleshow/38891225.cms.

19. Ramasamy, S. M., Neelakantan, R., & Suresh, F. (2006). Predictive and modelling for landslides in the Nilgiris, South India using remote sensing and GIS. In R. K. Avasthy, B. Singh & R. Sivakumar (Eds.), *Landslides perception and initiatives of DST* (pp. 177–203) Kolkata: Indian Society Engineering Geology.

20. GSI Report. (2006). Geology and mineral resources of the states of India. Part IV-Tamil Nadu and Pondicherry.

21. GSI. (1995). Geological and mineral map of Tamil Nadu and Pondicherry. Published in 1:500,000 scale by the Director General, Geological Survey of India.

22. Ayalew, L., Yamagishi, H., Marui, H., & Kanno, T. (2005). Landslides in Sado Island of Japan: part II. GIS-based susceptibility mapping with comparisons of results from two methods and verifications. *Engineering Geology, 81*(4), 432–445.

23. Hasekiogullari, G. D., & Ercanoglu, M. (2012). A new approach to use AHP in landlside susceptibility mapping: A case study at Yenice (Karbuk, NW Turkey). *Natural Hazards, 63,* 1157–1179.

24. Ramesh, V., & Anbazhagan, S. (2015). Landslide susceptibility mapping along Kolli hills Ghat road section (India) using frequency ratio, relative effect and fuzzy logic models. *Environmental Earth Sciences, 73*(12), 8009–8021.

25. Sujatha, E. R., Rajamanickam, G. V., & Kumaravel, P. (2012). Landslide susceptibility analysis using probablistic certainty factor approach: A case study on Tevankarai stream watershed, India. *Journal of Earth System Sciences, 121*(5), 1337–1350.

26. Ercanoglu, M., & Gokceoglu, C. (2004). Use of fuzzy relations to produce landslide susceptibility map of a landslide prone area (West Black Sea Region, Turkey). *Engineering Geology, 75,* 229–250.

27. Jenks, G. F. (1967). The data model concept in statistical mapping. *International Year Book of Cartography, 7,* 186–190.

28. Meten, M., Bhandary, N. P., & Yatabe, R. (2015). Effect of landslide factor combinations on the prediction accuracy of landslide susceptibility maps in the Blue Nile Gorge of Central Ethiopia. *Geoenvironmental Disasters, 2,* 9.

29. Anbazhagan, S., & Ramesh, V. (2014). Landslide hazard zonation mapping in ghat road section of Kolli Hills, India. *Journal of Mountain Science, 11*(5), 1308–1325.

30. Jaiswal, P., van Westen, C. J., & Jetten, V. (2010). Quantitative landslide hazard assessment along a transportation corridor in southern India. *Engineering Geology, 116,* 236–250.

31. Sajinkumar, K. S., & Anbazhagan, S. (2015). Geomorphic appraisal of landslides on the windward slope of Western Ghats, southern India. *Natural Hazards, 75*(1), 953–973.

32. Lee, S., & Talib, J. A. (2005). Probabilistic landslide susceptibility and factor effect analysis. *Environmental Geology, 47,* 982–990.

33. Park, S., Choi, C., Kim, B., & Kim, J. (2013). Landslide susceptibility mapping using frequency ratio, analytic hierarchy process, logistic regression, and artificial neural network methods at the Inje area, Korea. *Environmental Earth Sciences, 68*(5), 1443–1464.

34. Saaty, T. L. (1980). *The analytical hierarchy process: Planning, priority setting, resource allocation*. New York: McGraw Hill.

35. Yalcin, A. (2008). GIS-based landslide susceptibility mapping using analytical hierarchy process and bivariate statistics in Ardesen (Turkey): Comparisons of results and confirmations, Turkey. *CATENA, 72,* 1–12.

36. Wu, Y., Li, W., Liu, P., Bai, H., Wang, Q., He, J., et al. (2016). Application of analytic hierarchy process model for landslide susceptibility mapping in the Gangu County, Gansu Province, China. *Environmental Earth Sciences, 75,* 422.

37. Thanh, L. N., & De Smedt, F. (2012). Application of an analytical hierarchical process approach for landslide susceptibility mapping in A Luoi district, Thua Thien Hue Province, Vietnam. *Environmental Earth Sciences, 66*(7), 1739–1752.

38. Chung, C.-J. F., & Fabbri, A. G. (1999). Probabilistic prediction models for landslide hazard mapping. *Photogrammetric Engineering and Remote Sensing, 65*(12), 1389–1399.

39. Xu, C., Xu, X., Dai, F., Wu, Z., He, H., Shi, F., et al. (2013). Application of an incomplete landslide inventory, logistic regression model and its validation for landslide susceptibility mapping related to the May 12, 2008 Wenchuan earthquake of China. *Natural Hazards, 68,* 883–900.

40. Fawcett, T. (2006). An introduction to ROC analysis. *Pattern Recognition Letters, 27,* 861–874.